01 Jan 2001

Amplitude Modulated Droplet Formation in High Precision Solder Droplet Printing

Qingbin Liu

M. Orme

Ming-Chuan Leu
Missouri University of Science and Technology, mleu@mst.edu

Recommended Citation

Q. Liu et al., "Amplitude Modulated Droplet Formation in High Precision Solder Droplet Printing," *Proceedings of the International Symposium on Advanced Packaging Materials: Processes, Properties and Interfaces, 2001*, Institute of Electrical and Electronics Engineers (IEEE), Jan 2001.
The definitive version is available at https://doi.org/10.1109/ISAOM.2001.916561

Amplitude Modulated Droplet Formation in High Precision Solder Droplet Printing

Qingbin Liu, Ming C. Leu
Mechanical & Aerospace Engineering & Engineering Mechanics Department
University of Missouri-Rolla, MO65409-0050
Melissa Orme
Mechanical & Aerospace Engineering Department
University of California-Irvine, CA92697-3975

ABSTRACT

There are many methods used today to apply solder to wafers, ceramics, laminate and flex circuit boards and other substrates. Among these, high-precision solder droplet printing technology, which is non-contact, data driven, flexible and environmentally friendly, is a key enabling technology. This technology selectively deposits solder droplets only where required, therefore, needs no mask or secondary resist removal, uses materials more efficiently and creates less waste than other methods. Currently, continuous droplet formation from capillary streams is mainly achieved by the application of well-known Rayleigh instability in which a sinusoidal disturbance is applied to the stream which results in evenly spaced and sized droplets. However, changing droplet configurations for various products or varying the size or depth of solder joints is difficult. Amplitude modulated disturbance is employed in this work to generate arbitrary solder stream configurations. The final configuration is mainly determined by the following parameters: 1) the degree of modulation of the waveform; 2) the phase difference between the carrier and modulation signals; 3) the charging voltage; and 4) the frequency ratio between the carrier signal and the modulation signal. Many different patterns can be achieved with the proper combination of frequency ratio, phase difference, degree of modulation, and charging voltage. A simulation code was developed to simulate the merging process and determine the parameters needed to achieve certain droplet configuration.

Keywords: Solder Droplet Printing, Arbitrary Amplitude Modulated Droplet Formation, Microelectronics

1. INTRODUCTION

There are many methods used today to apply solder to wafers, ceramics, laminate and flex circuit boards and other substrates. Among these, high precision solder droplet printing technology, which is non-contact, data-driven, flexible and environmentally friendly, is a key enabling technology [1]. This technology, as shown in Fig.1, selectively and precisely deposits solder droplets only where required, therefore, needs no mask or secondary resist removal, uses materials more efficiently, and creates less waste than other methods.

The ability to place material fast and accurately makes the solder droplet printing technology a must evaluate tool for current and future microelectronic industry. Solder droplet printing will provide the microelectronic industry with a technique to address, in a cost-effective manner, the continuing pressures for miniaturization and higher performance and at the same time will enable new packaging designs and is suitable for a variety of applications including direct chip attach site preparation, 3-D substrates, fine line interconnect, substrate via fill, optoelectronics and many others. It would also allow manufacturing techniques that are impossible or unfeasible with current technology, such as localized replacement of solder on board (for rework or custom connections), depositing solder in different thickness on the same board (components differ in the amount of solder required for the best connection), or using more than one type of solder on the same board (temperature-sensitive components could be attached with lower-temperature solder after other components already are in place).

The solder droplet printing technology can be divided into two categories: continuous solder droplet printing and the drop-on-demand solder droplet printing [2]. Here we focus on the continuous solder droplet printing technology. Continuous droplet formation from capillary streams is mainly achieved by the application of well-known Rayleigh instability in which a sinusoidal disturbance is conventionally applied to the stream which results in evenly spaced and sized droplets as shown in Fig.2. Lord Rayleigh [3-5] discovered that application of a periodic disturbance on a capillary stream whose wavelength is greater than the circumference of the stream causes the radial disturbance to become unstable. The periodic vibration will translate to an unstable radial disturbance on the surface of the jet which grows until droplets are pinched from the stream. This ratio of the stream circumference to the disturbance wavelength is k_o^*, the non-dimensional wavenumber, which is

$$k_o^* = \frac{2\pi r_o}{\lambda} \quad (1)$$

where r_o is the orifice radius and λ is the wavelength of the applied disturbance. The surface waves grow exponentially in time as $e^{\beta t}$, where β is the growth rate for a viscous fluid given by Weber [6] as

$$\beta^2 + \frac{3\mu k_o^{*2}}{\rho r_o^2}\beta = \frac{\sigma}{2\rho r_o^3}(1-k_o^{*2})k_o^{*2} + \frac{v_s^2 \rho_a k_o^{*3} K_o(k_o^*)}{2\rho r_o^2 K_1(k_o^*)} \quad (2)$$

where K_n is the nth order modified Bessel function of the second kind, r_o is the unperturbed stream radius, ρ_a is the density of the ambient fluid, v is the kinematic viscosity of the fluid, σ is its surface tension, and k_o^* is defined above. Equation (2) predicts that the surface disturbance on a capillary stream is unstable and results in droplet formation for $k_o^*<1$, which agrees with experimental observations. Equation (2) also predicts that there is a maximum β at a k_o^*, denoted here as $k_{o\,\max}^*$.

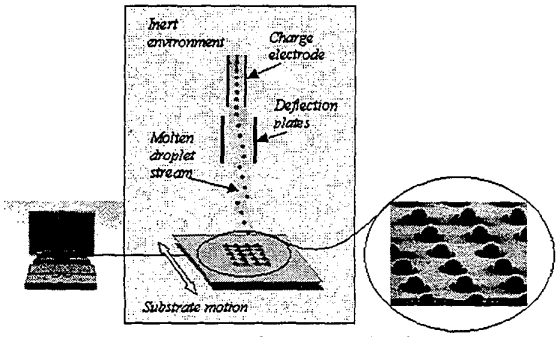

Figure 1: Schematic of the solder droplet printing.

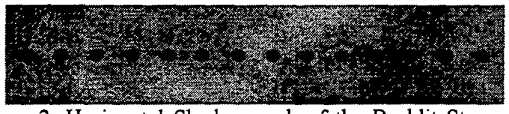

Figure 2: Horizontal Shadowgraph of the Backlit Stream of Droplets Perturbed by the Conventional Sinusoidal Disturbance.

Recent experimental studies have been conducted to investigate the production of uniformly sized droplets and on the nonlinear effects of capillary growth [7-10]. However, changing droplet configurations for various products or varying the size or depth of solder joints is difficult. Amplitude modulated disturbance is employed in this work to generate arbitrary solder stream configurations. In this paper, the theoretical basis for the amplitude modulated droplet formation is introduced, the effect of various parameters on the final configuration of the droplet stream is analyzed, and a simulation code is developed to simulate the merging process and determine the parameters needed to achieve certain droplet configuration.

2. ARBITRARY AMPLITUDE MODULATED DROPLET FORMATION

When an oil capillary stream is perturbated with an amplitude modulated sinusoidal waveform, the droplet stream undergoes a unique breakup and coalescence process that was first observed by Orme and Muntz [11,12]. The stream initially breaks into droplets that are separated by a distance commensurate with the frequency of the disturbance. While traveling downstream, the droplets from the two adjacent half periods of the modulation cycle eventually merge to form one large droplet. In order to increase the flexibility of droplet formation from capillary stream break-up, the forcing disturbance that has the form of an amplitude-modulated waveform can be applied. Use of the amplitude-modulated disturbance will extend the droplet separation and droplet diameters beyond that allowed by the conventional Rayleigh breakup, and will allow the droplet stream to be composed of more than one droplet size at predictable separations. This is due to the controlled merging of droplets in flight. An amplitude-modulated signal is composed of two sinusoidal signals: the carrier signal, which is the highest power signal, and the modulation signal, which corresponds to the relatively weaker sidebands. Such an amplitude-modulated pressure disturbance can be generated by the equation

$$p(t) = p_o + \Delta p(1+\alpha \sin \omega_m t)\sin(\omega_c t + \phi_c) \quad (3)$$

where p_o is the stagnation pressure that drives the mean fluid flow through the orifice, Δp is the amplitude of the fluctuating pressure disturbance, t is the time, α is the degree of modulation of the waveform, ϕ_c is the phase difference between the carrier and modulation signals, ω_m and ω_c are the modulation and carrier frequencies respectively, so that the frequency ratio between the carrier signal and the modulation signal, R, is equal to ω_c/ω_m.

When a fluid stream is perturbed with an amplitude-modulated disturbance whose carrier frequency is in the range of Rayleigh growth, the disturbance will be unstable and initial droplets will be formed with sizes and separations commensurate with the carrier disturbance, and hence are termed "carrier" droplets. Unlike conventional droplet formation, the droplets initially formed have relative velocities, Δu, which are a result of the asymmetry of the forcing disturbance. The component of the model which describes the attainment of the relative velocity of the ith droplet due to the asymmetry of the forcing distance, Δu_i, is based on

Rayleigh's linear theory that states that the stream's radius $r(t)$ grows in time t as:

$$r(t) - r_0 = \pm r_0 \kappa_0 e^{\beta t} \quad (4)$$

where κ_0 is the initial amplitude of the disturbance, r_o initial unperturbed stream radius, β disturbance growth rate. The following transfer function that relates the time varying pressure disturbance $p(t)$ to the radial perturbation on the stream has been shown to give adequate estimates of the impulse exerted on the stream:

$$\frac{r(t)}{r_0} = 1 \pm \{[p(t)/p_0]^{1/4} - 1\} e^{\beta t} \quad (5)$$

The impulse exerted on each drop as a result of the disturbance has been estimated by using momentum balance and conservation of mass. In this case, the momentum balance is applied about the remaining necking point of a drop to be formed. With the assumption that the pressure of the liquid at the break points is dominated by surface tension, the relative speed of each droplet can be estimated from:

$$\Delta u_i = \frac{1}{m_i} \int_{t_{bi}}^{t_{bi+1}} \pi \sigma r(t) dt \quad (6)$$

where m_i is the mass of the ith droplet, t_{bi} and t_{bi+1} are the break times of the forward and rearward extremes of the potential droplet, σ is the surface tension of the molten solder. Depending on the characteristics of the amplitude-modulated disturbance, such as frequency ratio and phase difference, the droplets may acquire a component of velocity relative to the average stream speed. The relative velocity causes the 'carrier droplet' to eventually collide with its neighbor, forming what is called the 'modulation droplet'. Monodisperse droplet streams at extended wavelengths may be generated this way, as well as droplet streams with predictable sequences of repeating patterns with different size droplets. This is done by varying the frequency ratio, phase difference, and so on.

As discussed above, amplitude modulated droplets acquire a relative velocity that cause them to collide with their neighbors. If the droplets are charged, however, they will attract or repel one another according to the equation

$$\Delta \tilde{u}_i = \frac{1}{4\pi\varepsilon_o m_i} \int_t^{t'} \sum_j^M \frac{Q_j Q_i}{r_{ij}^2} dt \quad (7)$$

Here, the mutual interactions between M droplets are considered. r_{ij} is the instantaneous distance between drops with index i and j that have charges Q_i and Q_j respectively. The limits of integration, t and t' correspond to the time at which the "tracking" of droplet trajectories is initiated, and the time when either all of the droplets merge into their final configuration of modulation drops or undergo one complete oscillation cycle, whichever the case may be, respectively. The relative droplet speeds at a specific instant time are the sum of $\Delta \tilde{u}_i$ and Δu_i given by Eq.(6) and Eq.(7) respectively.

Generation of the above droplet stream configurations without the amplitude modulation is impossible with the Rayleigh mode of droplet formation. This is because the equivalent non-dimensional wavenumber k_o*, which is needed to generate the streams, would be out of the range of k_o*'s for uniform droplet formation, yielding a highly irregular droplet stream with nonuniform sizes and separations. In fact, the droplet streams generated with the amplitude-modulated disturbances are more uniform than the conventional Rayleigh-mode droplets. Orme *et al.* [12] found that the speed dispersion of amplitude-modulated disturbances decreases as $1/R$, where R is the frequency ratio of the amplitude-modulated disturbance. Droplet streams generated with amplitude-modulated disturbances are beneficial for use with net-form materials synthesis, since they allow highly uniform droplet generation at extended wavelengths.

3. MODELLING

In order to determine whether charged droplets may be merged to form modulation droplets, Eq.(6) and Eq.(7) were used in a simulation based on the conservation of momentum to track the droplets in flight while taking into account electrostatic interactions. Parameters such as the number of droplets to track and flight distance, as well as stream diameter and disturbance waveform characteristics are input at the beginning of the simulation. From the growth rate β and the shape of the pressure disturbance ε applied at the orifice, the break time for each droplet, t_b, is calculated using the following equation

$$t_b = \frac{-\ln \varepsilon}{\beta} \quad (8)$$

Once the break times are calculated, the initial conditions of each droplet can be calculated, which includes the droplet mass, radius, position, velocity, and charge. As such, the stream is no longer treated as droplets generated one by one from the breakup of an unstable stream, but as a pre-existing train of droplets issuing from a virtual source located at the orifice position. This simplifies the tracking process for the section where the droplets have not yet traveled the distance from the orifice to the break point.

After new droplet positions are calculated, inter-droplet spacings are checked to see if two adjacent droplets come within a center-to-center spacing of their equivalent diameter. The equivalent diameter is determined by the sum of the radii of each droplet. If so, the mass, charge, and momentum of the two

droplets are added. The center of the mass of the droplet train being tracked is then determined for data display purpose. After these calculations are completed, another time-step is taken and the calculation procedure repeats itself. This is done until the leading droplet travels a predetermined distance (usually the distance to the substrate in the experimental setup). Afterward the final droplet stream configuration is written to a data file. At the end of the simulation a high resolution trace of the applied pressure disturbance is generated for data display purpose.

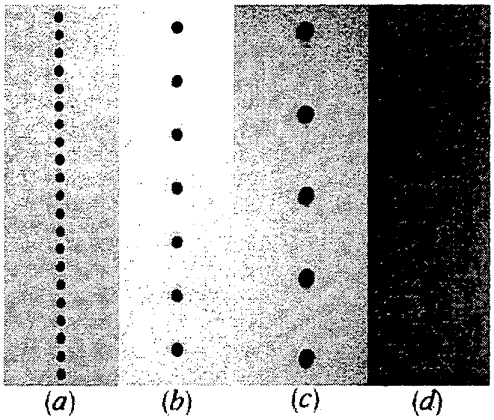

Figure 3: Final configurations of the amplitude modulated droplet stream for a) conventional droplets, b) droplets generated with R=3, c) droplets generated with R=4, d) droplets generated with R=3.5.

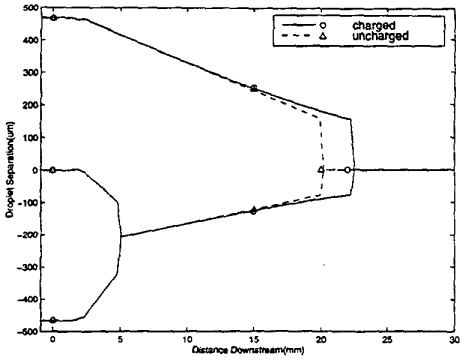

Figure 4: Simulation and experimental results for R=3, and α=40%.

4. RESULTS AND DISCUSSION

Different droplet stream configurations, where the spacing and the size of each droplet in the stream are varied in a predictable and controllable manner, have been achieved by using the methods described above.

When R is an integer, the relative velocities cause the droplets to merge systematically with their neighbors, resulting in "modulation" drops that are characterized by masses and wavelengths that are R times those of droplets generated with only the carrier disturbance as shown pictorially in photograph (b) and (c) of Fig.3. When R is not an integer, controlled polydispersed droplet stream as those shown in Fig.3(d) can be generated. In this case, the smaller droplets correspond to the unmerged "carrier" droplets and the larger drops result from systematic merging of several carrier drops.

Fig.4 illustrates the results from the model predictions and experiment for the case of droplets generated with an amplitude modulated disturbance with R=3 and α=40%. The solid and dashed lines represent the charged and uncharged conditions respectively in the simulations, and the circle and triangle symbols represent the charged and uncharged experimental results respectively. The abscissa is the distance downstream of the droplet formation point that results in the shown configuration. The ordinate is the droplet separation measurement for the droplet packet under investigation. As can be seen, the three droplets are originally separated a distance of 475μm. As they travel downstream, they begin to systematically merge until they ultimately form modulation drops. In this case, the effect of droplet charge is to increase the distance required to achieve complete droplet merging by approximately 2 mm. The small effect of droplet charge is due to the fact that the degree of modulation, α, is relatively high which causes the component of the relative droplet speed arising from the lack of symmetry of the forward and backward break-times of the droplet to be much higher than the relative speed due to the droplet charge interactions, i.e., $\Delta u > \Delta\tilde{u}$. When the degree of modulation is lower, the component of the relative speed due to the amplitude-modulated disturbance will be commensurate with that due to electrostatic interactions, and hence greater differences between the charged and uncharged trajectories will appear.

As comparison, Fig.5 illustrates the model simulations for the case when R=3 and α=10%. The solid line represents charged droplets and the dashed line represents the case of uncharged droplets. In the uncharged case, the merging distance is larger than 500mm as shown in the figure. The large merging distance is due to the fact that the relative velocities of the droplets are small due to the weakly modulated disturbance. Since in this case the droplets are uncharged, there is no force which would cause their relative velocities to deviate from their original values, and hence the gradient of their relative positions would be constant as shown, ultimately resulting in a stream of modulation drops far from the orifice. However, when the droplets are charged, the electrostatic interactions prohibit droplet merging, as can be seen by the solid oscillating lines in Fig.5. As the separation between droplets decreases due to their relative velocities, the

electrostatic force causes them to repel from each other, thereby increasing their separation. Since the droplets are in an infinite stream, the neighbor droplets on each side prohibit extreme excursions from their original relative spacing, thereby causing the measured oscillatory behavior.

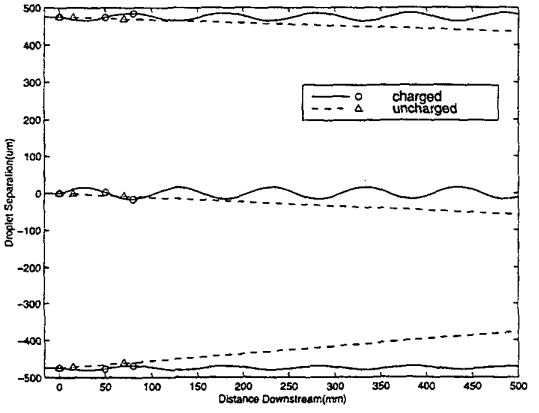

Figure 5: Simulation and experimental results for R=3, and α=10%.

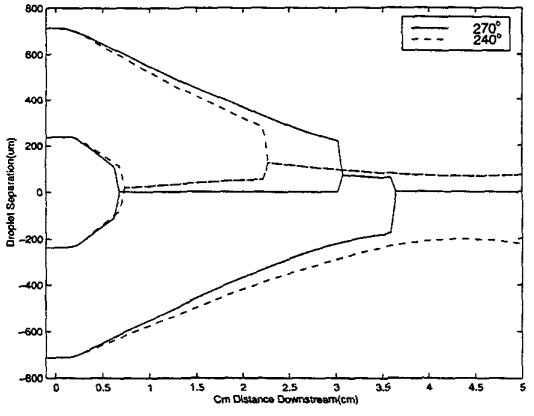

Figure 6: Simulation of droplet merging for R=4, α=40%, and Vc=100V.

The phase difference between the carrier signal and modulation signal is another important factor to influence the disturbance waveform so that it eventually influence the final configurations of droplet stream. To illustrate this, the final confiurations of droplet streams are simulated with R=4, α=40% and Vc=100V. Fig.6 illustrates simulation results taken with the ϕ_c =270° and the dashed line represents the stream with ϕ_c being 240°. It can be seen that the droplets are completely merged by approximately 36mm in the case of ϕ_c =270°. While in the case of ϕ_c =240°, only the first three droplets merge, however the fourth droplet in the packet is repelled and hence, the droplet stream never completely merges. Rather, the final droplet stream will be large-small, large-small model.

From the discussion above, it can seen that the droplet stream configurations are mainly influenced by the following parameters:1) α, the degree of modulation of the waveform; 2) ϕ_c, the phase difference between the carrier and modulation signals; 3) V_c, the charging voltage; and 4) R, the frequency ratio between the carrier signal and the modulation signal. Different kind of droplet configurations could be achieved through the combination of the aforementioned parameters.

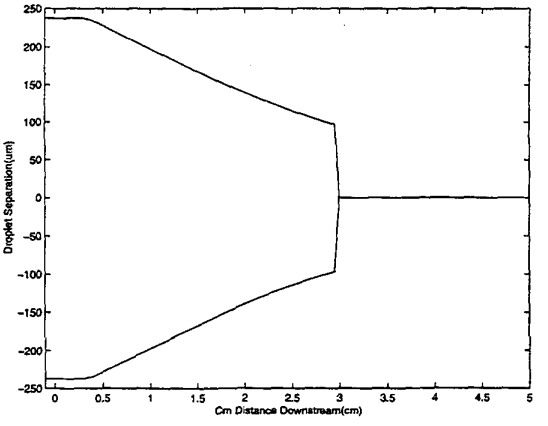

Figure 7: Simulation of droplet merging for R=2, α=50%, Vc=100V, and ϕ_c=100°.

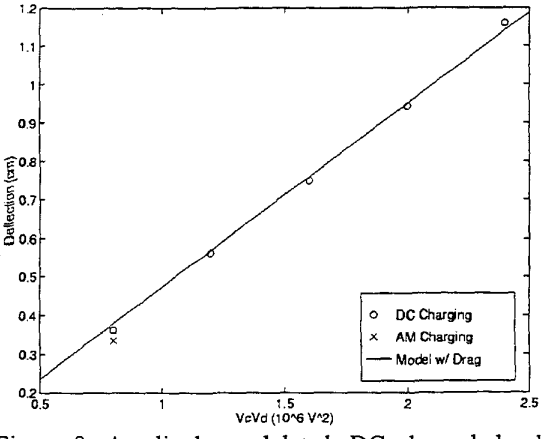

Figure 8: Amplitude modulated, DC charged droplet deflection experimental and predicted results.

The simulation model developed by the authors can also be used to predict the degree of modulation, phase difference, and other parameters required to merge a modulation packet of droplets at a fixed distance downstream from the orifice. For example, in the case

of R=2, two small droplets merged into a large one at a distance of about 3cm downstream from the orifice is required. Through the simulations using different degree of modulation and phase difference, this case would be achieved with α=50% and ϕ_c=100°. Fig.7 illustrates the simulation result of this case. As can be seen, the two small droplets have merged into a large one about 3cm downstream from the orifice. So, the model developed here could be used to optimize the parameters to achieve the desired pattern configurations.

Once the charged droplets are completely merged, they can be deflected exactly as the conventional droplets generated with a sinusoidal disturbance are deflected. When the droplets generated with amplitude-modulated disturbances coalesce to form their final configuration, the final droplet mass is the sum of all of the merged droplet masses, and the final droplet charge is the sum of all of the charges of the merged droplet charges. Hence, the charge-to-mass ratio of the drops in the final stream configuration will be the same as in the unmerged configuration. Fig.8 shows the experimental deflection of amplitude-modulated droplets as compared to the deflection of carrier droplets making up the modulation droplet. The deflection of the modulation droplet consisting of four carrier droplets falls approximately on the same line as the deflection of the carrier droplets, although it undergoes eight percent less deflection. The "x" symbol in Fig.8 represents the deflection of the modulation droplets.

5. CONCLUSION

The ability to place material fast and accurately makes the solder droplet printing technology a must evaluate tool for current and future microelectronic industry. Currently, continuous droplet formation from capillary streams is mainly achieved by the application of well-known Rayleigh instability in which a sinusoidal disturbance is conventionally applied to the stream which results in evenly spaced and sized droplets. However, changing droplet configurations for various products or varying the size or depth of solder joints is difficult. Amplitude modulated disturbance is employed in this work to generate arbitrary solder stream configurations. In this paper, the theory basis for the amplitude modulated droplet formation was introduced, the effect of various parameters on the final configuration of the droplet stream was analyzed, and a simulation code was developed to simulate the merging process and determine the parameters needed to achieve certain droplet configuration. The final configuration is mainly determined by the following parameters: 1) the degree of modulation of the waveform; 2) the phase difference between the carrier and modulation signals; 3) the charging voltage; and 4) the frequency ratio between the carrier signal and the modulation signal. Many different patterns can be achieved with the proper combination of frequency ratio, phase difference, degree of modulation, and charging voltage.

REFERENCE

[1] Qingbin Liu, M.C. Leu, Melissa Orme, High Precision Solder Droplet Printing Technology: Principle and Applications, To be presented in the International Symposium and Exhibition on Advanced Packaging Materials: Processes, Properties and Interfaces, March11-14, 2001, Braselton, Georgia

[2] Richard Godin, Metal Jet Bumping and Application, Nepcon Texas Proceedings, Texas, USA, October, 1997

[3] Lord Rayleigh, On the Instability of Jets, Proceedings of the Royal Society of London, Mathematics,10:4-13, November 1878.

[4] K. Chaudhary and L. Redekopp, The nonlinear capillary instability of a liquid jet, part 1: theory, Journal of Fluid Mechanics, 1980, 96(2):257-274.

[5] K. C. Chaudhary and T. Maxworthy, The nonlinear capillary instability of a liquid jet, part 2: experimental on jet behavior before droplet formation, Journal of Fluid Mechanics, 1980, 96(2):275-286.

[6] Weber, C., Zum zerfall eines flussigkeitsshahies, *Z. Angew. Math. Mech.*, 1931, 11(2), pp.136-154.

[7] Goedde, E. F., Yuen, M. C., Experiments of Liquid Jet Instability, Journal of fluid mechanics, 1970,40(3), pp.495-511.

[8] Schneider, J.M, Linblad, N.R., Hendricks, C.D., and Crowley, J.M., Stability of an Electrified Liquid Jet, Journal of applied Physics, 1967, 38(6), pp.2599-2606.

[9] Yuen, M.C., Non-linear Capillary Instability of a Liquid Jet, Journal of Fluid Mechanics, 1968, 33(1) , pp.151-163.

[10] Taub, H. H., Investigation of Nonlinear Waves on Liquid Jets, The physics of fluids, 1976, 18(8), pp.1124-1129.

[11] Orme, M., and Muntz, E. P., New Technique for Producing highly uniform droplet streams over an extended range of disturbance, The Review of Scientific Instruments, 1987, 58(2), pp.279-284.

[12] Orme, M. and Muntz, E. P., The Manipulation of Capillary Stream Breakup Using Amplitude-modulated Disturbances: A Pictorial and Quantitative Representation, Phys. Fluids, v2(7), 1990, pp.1124-1140.